Analytical solution of Mori's equation with hyperbolic secant memory

1994 J. Phys.: Condens. Matter 6 591

(http://iopscience.iop.org/0953-8984/6/3/002)

J. Phys.: Condens. Matter 6 (1994) 591–602. Printed in the UK

Analytical solution of Mori's equation with hyperbolic secant memory

K Tankeshwar†§ and K N Pathak‡

† International Centre for Theoretical Physics, Trieste 34100, Italy

‡ Centre of Advanced Study in Physics, Department of Physics, Panjab University, Chandigarh 160014, India

Received 3 August 1993, in final form 25 October 1993

Abstract. The equation of motion of the auto-correlation function has been solved analytically using a hyperbolic secant form of the memory function. The analytical result obtained for long-time expansion together with short-time expansion provides a good description over the whole time domain as judged by a comparison with the numerical solution of the Mori equation of motion. We also find that the time evolution of the auto-correlation function is determined by a single parameter τ which is related to frequency sum rules up to fourth order. The auto-correlation function has been found to show simple decaying or oscillatory behaviour depending on whether the parameter τ is greater than or less than some critical value. Similarities as well as differences in the time evolution of the auto-correlation have been discussed for exponential, hyperbolic secant and Gaussian approaches of the memory function.

1. Introduction

A considerable amount of work has been carried out in recent years to study the time evolution of auto-correlation functions (ACFs) and transport coefficients of atomic fluids. In these studies, equilibrium [1, 2] and non-equilibrium [3–6] molecular dynamics techniques have been used to investigate velocity, stress and energy current density ACFs. On the other hand, the ACFs can be studied theoretically [7] through Mori's integro-differential equation. In this approach, the fundamental theoretical quantity to be calculated is the memory function. The reduction of the problem of studying ACFs to calculate the appropriate memory function is an important step in the theoretical analysis of atomic motion in fluids. Since the exact microscopic calculation of the memory function is not yet feasible, in general, simple approximations to the memory function can be made that preserve a number of important properties of the ACF irrespective of the approximation introduced for the memory function. In the present work, we use a hyperbolic secant form of the memory function, which is a solution of a non-linear differential equation well known to soliton dynamics. This memory function has been used by us [8–11] and also by Heyes and Powles [12] in the study of time correlation functions (TCFs) and transport coefficients of classical dense fluids and has provided a very satisfactory agreement with the available computer simulation data. In fact, very recently Leegwater [13] has derived an expression for the first-order memory function of the velocity ACF using the kinetic theory approximation, fitted to the hyperbolic secant form. However, in all the earlier studies of the time correlation function using hyperbolic secant memory the underlying Mori equation has been solved only numerically. Therefore,

§ Permanent address: Department of Physics, HP University, Shimla-171005, India.

0953-8984/94/030591+12$07.50

the aim of the present study is to solve analytically the Mori equation with hyperbolic secant memory. The analytical solutions provide a clearer picture of the time evolution of the ACFs as has also been demonstrated by Denner and Wagner [14] using exponential and Gaussian memory functions.

The layout of the paper will be as follows. In section 2 we introduce the memory function used in this work. In section 3, we discuss the Fourier spectrum of the ACF. The analytical short- and long-time expansions for the ACF are obtained in section 4. Section 5 contains an analytical investigation of the poles of the Laplace transform of the ACF. The validity of analytical expressions for the poles is also checked in this section by comparing with numerical results. In section 6, we compare our analytical results with that obtained from numerical calculation of the ACF. In section 7, the results of the ACF obtained with hyperbolic secant memory are compared with those obtained with Gaussian and exponential memory.

2. The model memory function

Mori has shown that ACFs obey an equation of motion [7] that determines their time evolution. It is given by

$$\frac{\mathrm{d}C(t)}{\mathrm{d}t} + \int_0^t C(t')M_1(t-t')\,\mathrm{d}t' = 0 \tag{1}$$

where $C(t)$ is the ACF of some dynamical variable $A(t)$. $M_1(t)$ is the first-order memory function and is defined as

$$M_1(t) = \langle f_1(t) f_1^*(0)\rangle / \langle |f_1(0)|^2\rangle \tag{2}$$

where

$$f_1(t) = \exp(\mathrm{i}Q_1 L Q_1 t) Q_1 A.$$

The operator Q_1 $(= 1 - P_1)$ projects onto the subspace orthogonal to the variable $A(t)$. The angular brackets in (2) represent the ensemble average and L is the Liouville operator. In order to calculate the time evolution of the ACF from (1), the fundamental theoretical quantity needed is the memory function $M_1(t)$. If we apply the projection operator technique used in deriving (1) to the case when $f_1(t)$ is treated as the dynamical variable, we obtain an equation similar to (1) for the time evolution of $M_1(t)$. This provides

$$\frac{\mathrm{d}M_1(t)}{\mathrm{d}t} + \int_0^t M_1(t')M_2(t-t')\,\mathrm{d}t' = 0 \tag{3}$$

where $M_2(t)$ is the second-order memory function defined as

$$M_2(t) = \langle f_2(t) f_2^*(0)\rangle / \langle |f_2(0)|^2\rangle \tag{4}$$

with

$$f_2(t) = \exp(\mathrm{i}Q_2 L Q_2 L) Q_2 f_1 \qquad Q_2 = 1 - P_1 - P_2$$

and the operator P_2 projects on ordinary dynamical variable $f_1(t)$. We differentiate (3) with respect to time t to obtain

$$\frac{d^2M_1(t)}{dt^2} + b^2M_1(t) + \int_0^t \frac{dM_2(t-t')}{dt} M_1(t')\,dt' = 0 \tag{5}$$

where $M_2(0) = b^2 = \delta_2 = (C_4/C_2 - C_2)$ with C_{2n} being the nth-order sum rule of the ACF defined as

$$C_{2n} = \left\langle \frac{d^nA(t)}{dt^n} \frac{d^nA(t)}{dt^n} \right\rangle_{t=0} \Big/ \langle A^2(0)\rangle.$$

Now the problem of calculating the time development of the ACF reduces to the calculation of $M_2(t)$ or $M_1(t)$, which themselves are time correlation functions of time derivatives of the original dynamical variable $A(t)$. The exact microscopic calculation of $M_1(t)$ or $M_2(t)$ is not yet possible. Therefore, several phenomenological forms of the memory function have been proposed in the literature [7–12]. In this work we take

$$M_1(t) = a\ \mathrm{sech}(bt) \tag{6}$$

with $a = M_1(0) = \delta_1 = C_2$. This memory function tends to Gaussian and simple exponential forms for the short and long times, respectively. It is also noted that $M_1(t)$ given by (6) is a solution of a non-linear differential equation, well known in soliton dynamics, given by

$$d^2M_1(t)/dt^2 - b^2M_1(t) + (2b^2/a^2)M_1^3(t) = 0. \tag{7}$$

The analytical results obtained for the time correlation function using the hyperbolic secant memory function is expected to demonstrate the effect of the non-linearity reflected through (7) of the atomic motion on the time evolution of the ACF.

3. Power spectrum of the auto-correlation function

In order to calculate the time evolution of the ACF $C(t)$ and its power spectrum we rewrite (1) as

$$\frac{dC(\hat{t})}{d\hat{t}} + \frac{2}{\pi\tau} \int_0^t \mathrm{sech}(\epsilon) C(\hat{t} - \xi)\,d\xi = 0 \tag{8}$$

where the reduced time scale is $\hat{t} = \sqrt{\delta_2}t$ and

$$\tau = (2/\pi)(\delta_2/\delta_1). \tag{9}$$

In (8) we have used the memory function as given by (6). It may be noted that now the ACF involves only one essential parameter τ. During the Laplace transform as

$$\tilde{C}(z) = \int_0^\infty \exp(-z\hat{t})C(\hat{t})\,d\hat{t} \tag{10}$$

we obtain

$$\tilde{C}(z) = 1 \Big/ \left[z + \frac{2}{\pi\tau}\beta\left(\frac{z+1}{2}\right)\right] \tag{11}$$

where

$$\beta\left(\frac{z+1}{2}\right) = \int_0^\infty \operatorname{sech}(\hat{t}) \exp(-\hat{t}z)\, \mathrm{d}t$$

and has the series expansion [15]

$$\beta(x) = \sum_{k=0}^{\infty} \frac{(-1)^k}{x+k}. \tag{12}$$

The Fourier transform $G(\omega)$ of the ACF $C(t)$ is related to its Laplace transform $\tilde{C}(z)$ as

$$G(\omega) = \frac{1}{2\pi}\int_{-\infty}^{\infty} \mathrm{d}\hat{t} \exp(-\mathrm{i}\omega\hat{t})C(\hat{t}) = \frac{1}{\pi}\mathrm{Re}(\tilde{C}(\omega)). \tag{13}$$

Inserting (11) into (13), the power spectrum $G(\omega)$ is obtained as

$$G(\omega) = \frac{\tau}{\pi} \frac{\operatorname{sech}(\pi\omega/2)}{[\omega\tau + F(\omega)]^2 + \operatorname{sech}^2(\pi\omega/2)} \tag{14}$$

where

$$F(\omega) = \frac{\pi}{2}\tanh\left(\frac{\pi\omega}{2}\right) + \frac{1}{2}\left[\psi\left(\frac{1+\mathrm{i}\omega}{4}\right) - \psi\left(\frac{1-\mathrm{i}\omega}{4}\right)\right]. \tag{15}$$

In the above equation $\psi(x)$ is the Euler Psi function. We note that $F(\omega)$ has the expansions

$$F(\omega) = \frac{\omega}{4}\left(\pi^2 - \sum_{k=0}^{\infty}(\tfrac{1}{4}+k)^{-2}\right) - \left(\frac{\pi\omega}{2}\right)^3 \frac{\pi}{6}\cdots \tag{16}$$

for small ω and

$$F(\omega) = \frac{\pi}{2} - \frac{1}{2}\sum_{k=0}^{\infty} \frac{1}{\omega/4 + [(\frac{1}{4}+k)^2/\omega]4} \tag{17}$$

for large ω. Using (16) and the series expansion of $\operatorname{sech}(\pi\omega/2)$, we obtain the low-frequency behaviour of $G(\omega)$ as

$$G(\omega) = \frac{\tau}{\pi}\left\{1 + \frac{\pi^2}{8}\omega^2\left[1 - 2\left(\frac{2}{\pi}\tau + 1 - \frac{16}{\pi^2}\right)^2\right]\right\}. \tag{18}$$

However for large ω

$$G(\omega) = \frac{\tau}{\pi}\frac{\operatorname{sech}(\pi\omega/2)}{\tau^2\omega^2}. \tag{19}$$

It is evident from (18) and (19) that $G(\omega)$ will have a maximum for $\tau < \tau_m = (\pi/2)(1/\sqrt{2} - 1 + 16/\pi^2)^2 \simeq 2.1$. In figure 1, the power spectrum $G(\omega)$ of the ACF is shown over the entire frequency range for different values of τ. Following Denner and Wagner [14], we also find that the maximum in the power spectrum for $\omega > 0$ constitutes a sufficient condition for oscillatory decay of the ACF. In the next section it is shown that oscillatory behaviour of $C(t)$ is observed even for values $\tau > \tau_m$. This implies that the oscillatory behaviour of $C(t)$ is not a necessary condition for the existence of the peak in $G(\omega)$ at $\omega \neq 0$.

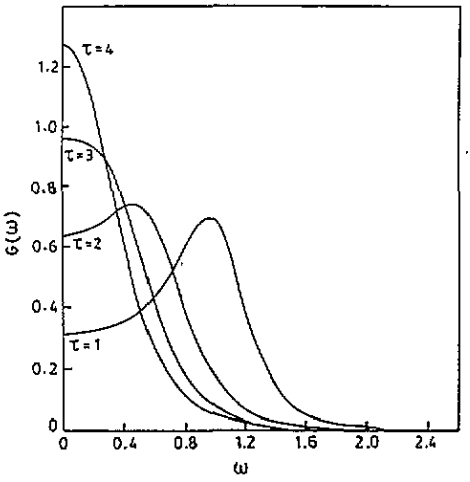

Figure 1. Fourier spectrum $G(\omega)$ of the ACF with sech(t) memory for different values of τ.

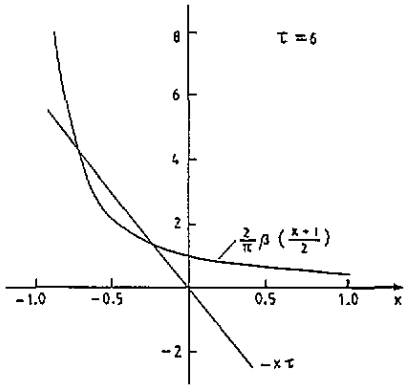

Figure 2. Graphical solution of (23) for real $z = x$. This determines the poles of $\tilde{C}(z)$ on the real axis.

4. Short- and long-time expansion for the auto-correlation function

The time evolution of $C(t)$ can be obtained by taking the inverse Laplace transform of (11) i.e.

$$C(\hat{t}) = \frac{1}{2\pi i}\int_{-i\infty}^{+i\infty} dz \exp(z\hat{t})\tilde{C}(z). \tag{20}$$

The short-time expansion of $C(\hat{t})$ is given by

$$C(\hat{t}) = 1 - \frac{2}{\pi\tau}\frac{t^2}{2} + O(t^4). \tag{21}$$

On the other hand, the long-time expansion of $C(\hat{t})$ is determined by evaluating the poles of $\tilde{C}(z)$ which are close to zero. In the next section, it is shown that there are two poles z_1 and z_2 in this region. The remaining poles give rise to terms that decay much faster. In view of the above fact and following the procedure of Denner and Wagner [14], we obtain the long-time expansion of (20) as

$$\frac{1}{2\pi i}\int_{-i\infty}^{+i\infty} dz \exp(z\hat{t})\tilde{C}(z)$$

$$= \frac{\exp(z_1\hat{t})}{1 + (1/\pi\tau)\beta'[(z+1)/2]|_{z=z_1}} + \frac{\exp(z_2\hat{t})}{1 + (1/\pi\tau)\beta'[(z+1)/2]|_{z=z_2}} \tag{22}$$

where $\beta'[(z+1)/2]$ is the first derivative of $\beta[(z+1)/2]$ with respect to z. This expansion is useful only if the poles z_1 and z_2 are known.

5. Investigations of the poles

5.1. General properties of the poles

The poles of $\tilde{C}(z)$ are given by the solution of the equation

$$f(z) = z + \frac{2}{\pi\tau}\beta\left(\frac{z+1}{2}\right) = 0. \tag{23}$$

In order to obtain the properties of the poles, we have solved (23) graphically for real z $(= x)$ as shown in figure 2. We observe the following: (i) the positive real axis is free of poles; (ii) for $\tau > \tau_c$ two poles exist near the origin on the negative real z axis; (iii) for $\tau = \tau_c$ the poles coincide and (iv) for $\tau < \tau_c$ no pole exists on the real axis. One can easily see from (22) that for $\tau < \tau_c$, the poles being in the complex z plane, the ACF shows oscillatory behaviour. For $\tau = \tau_c$ we have $z_1 = z_2 = x_c$ and obtain the conditions

$$f(x_c) = 0 \Rightarrow -\tau_c x_c = \frac{2}{\pi}\beta\left(\frac{x_c+1}{2}\right) \tag{24a}$$

and

$$f'(x_c) = 0 \Rightarrow -\tau_c = \frac{1}{\pi}\beta'\left(\frac{x_c+1}{2}\right). \tag{24b}$$

From (24*a*) and (24*b*), we find that

$$x_c\beta'\left(\frac{x_c+1}{2}\right) = 2\beta\left(\frac{x_c+1}{2}\right). \tag{25}$$

This equation can be solved numerically for x_c and hence for τ_c. We find that $x_c = -0.471\,39$ and $\tau_c = 4.4$. It may be noted that τ is an independent parameter and is related to the frequency sum rules, whereas z_1 and z_2 vary with τ. In order to have analytical dependence of z on τ we consider different regions of τ.

5.1.1. $\tau \gg \tau_c$. From figure 2 it can be seen that

$$\lim_{\tau\to\infty} z_1(\tau) = 0 \tag{26}$$

and

$$\lim_{\tau\to\infty} z_2(\tau) = -1. \tag{27}$$

Therefore, poles $z_1(\tau)$ may be obtained by expanding $f(z)$ and $z = 0$ up to terms of order z^2. The expression thus obtained is given as

$$z_1(\tau) = [-\tau_1\pi/\beta''(1/2)]\{1 - [1 - 2\beta'(1/2)/\pi\tau_1^2]^{1/2}\} \tag{28}$$

where $\tau_1 = \tau + \frac{1}{2}\beta''(1/2)$. On the other hand, the pole $z_2(\tau)$ is obtained by using expression (12) in (23):

$$z_2(\tau) = -\tfrac{1}{2} - \tfrac{1}{2}(1 - 16/\pi\tau)^{1/2}. \tag{29}$$

For very large values of τ, the contribution of pole $z_2(\simeq -1)$ to the ACF is negligible as seen from the expression (22), whereas $z_1(\tau) = 1/\tau$ for $\tau \to \infty$ is the leading term in (28). The resulting long-time expansion is given as

$$C(\hat{t}) = \exp(-\hat{t}/\tau). \tag{30}$$

Thus, for very large values of τ, the ACF $C(t)$ decays with a time constant τ. This result corresponds to $M_1(t) = (1/\tau)\delta(t)$ and agrees with that obtained from (1).

5.1.2. $\tau \geqslant \tau_c$. For $\tau = \tau_c$ we have $z_1(\tau_c) = z_2(\tau_c) = x_c$. Therefore, for slightly larger values of τ ($\geqslant \tau_c$), z_1 and z_2 can be derived from the series expansion of $f(z)$ around $x = x_c$. Using the relations (24*a*) and (24*b*), expressions are derived for z_1 and z_2:

$$z_1 = x_c - (2\tilde{\tau}/K)[1 - (1 - Kx_c/\tilde{\tau})^{1/2}] \tag{31}$$

$$z_2 = x_c - (2\tilde{\tau}/K)[1 + (1 + Kx_c/\tilde{\tau})^{1/2}] \tag{32}$$

with $\tilde{\tau} = \tau - \tau_c$ and $K = (1/\pi)\beta''[(x_c + 1)/2]$.

5.1.3. $\tau \leqslant \tau_c$. For $\tau \leqslant \tau_c$ no pole exists on the real axis. Taking the complex conjugate of (23) and noting that $\beta[(z^* + 1)/2] = \{\beta[(z + 1)/2]\}^*$, we see that the poles are always complex conjugate to each other. The condition is necessary for $C(t)$ to be real. As a result of the complex nature of the poles, oscillations occur in $C(t)$. Thus τ_c separates the region of oscillatory behaviour from that of monotonic decay of the ACF. The investigation of region $\tau \leqslant \tau_c$ involves a more detailed analysis, which is given in the appendix. There, we have obtained the approximate expressions for the poles $z_{1,2}(\tau) = x(\tau) \pm iy(\tau)$ with

$$x(\tau) = \tau_c x_c/\tau + (\tau - \tau_c)/\tau K' \tag{33}$$

and

$$y(\tau) = \left(\frac{24\pi(\tau - \tau_c)}{\beta'''[(x_c + 1)/2]}\right)^{1/2} \tag{34}$$

where $K' = \beta'''[(x_c + 1)/2]/6\beta''[(x_c + 1)/2]$.

For a more accurate description of the poles, one needs to solve the following differential equation obtained from (23):

$$\frac{dz(\tau)}{d\tau} = -\frac{z\tau}{\tau + (1/\pi)\beta'[(z + 1)/2]} \tag{35}$$

with $z = x + iy$.

5.1.4. $\tau \to 0$. In this region the poles tend to the imaginary axis and the ACF shows more oscillations. An analysis of this regime is also given in the appendix. Results are given as

$$x(\tau) = -(1/\tau)\ \mathrm{sech}(\pi/2\tau) \tag{36}$$

and

$$y(\tau) = -1/\tau. \tag{37}$$

In the next subsection, we check the validity of the above approximate expressions for the poles of $\tilde{C}(z)$.

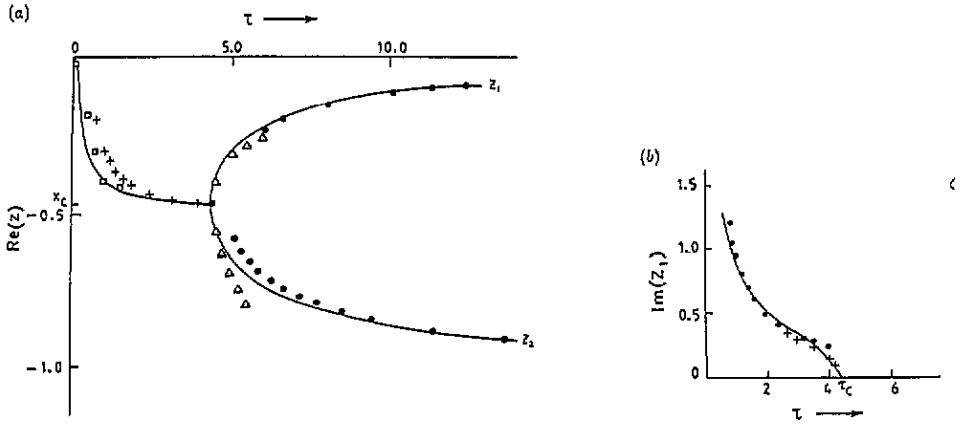

Figure 3. (*a*) Comparison between the numerically determined poles z_1 and z_2 and the approximate analytical expressions on the real z axis: solid curve, numerical solution; ●, values of z_1 and z_2 determined from (28) and (29); △, obtained from (31) and (32); +, obtained from (33); □, obtained from (36). (*b*) Comparison between the numerically determined imaginary parts of the poles ($\mathrm{Im}\, z_1 = -\mathrm{Im}\, z_2$): solid curve, numerical results; +, from (34); ●, from (37).

5.2. Estimation of validity

The validity of various analytical formulae derived in the previous subsection is checked by solving (23) numerically for z_1 and z_2. These numerically determined z_1 and z_2 along with their corresponding analytical values are shown in figure 3. From figure 3(*a*) it can be seen that (28) and (31) represent $z_1(\tau)$ very well. However, the pole $z_2(\tau)$ is not well described in the intermediate region $5 < \tau < 7$ by the analytical expressions (29) and (32). For this region, one may have to consider higher-order terms in the expansion. For $\tau < \tau_c$, we find that $x(\tau)$ and $y(\tau)$ are very well predicted by (33), (36) and (34), (37), respectively. On the whole, we find that our analytical expressions for the poles of $\tilde{C}(z)$ agree well with those obtained by numerical solution of (23) and, therefore, can be used to predict the long-time behaviour of the ACF using (22).

6. Comparison between numerical and analytical results for $C(t)$

The equation of motion (8) for the time evolution of the ACF can be solved numerically by taking the inverse Fourier transform of the power spectrum $G(\omega)$ i.e.

$$C(\hat{t}) = \frac{2}{\pi}\int_0^\infty G(\omega)\cos(\omega\hat{t})\,\mathrm{d}\omega. \tag{38}$$

The results obtained from (38) for $C(\hat{t})$ are shown as the full line in figure 4 for different values of τ. The results obtained from the long-time expansion (22) are also shown in figure 4 as solid circles. It can be seen from figure 4 that our analytical results give an overall good description of $C(\hat{t})$ if one excludes extremely short times. For the short-time region, the expansion (21) is applicable. Thus, both expansions taken together yield a good description of the time evolution of the ACF in the whole time domain for a wide range of parameter τ.

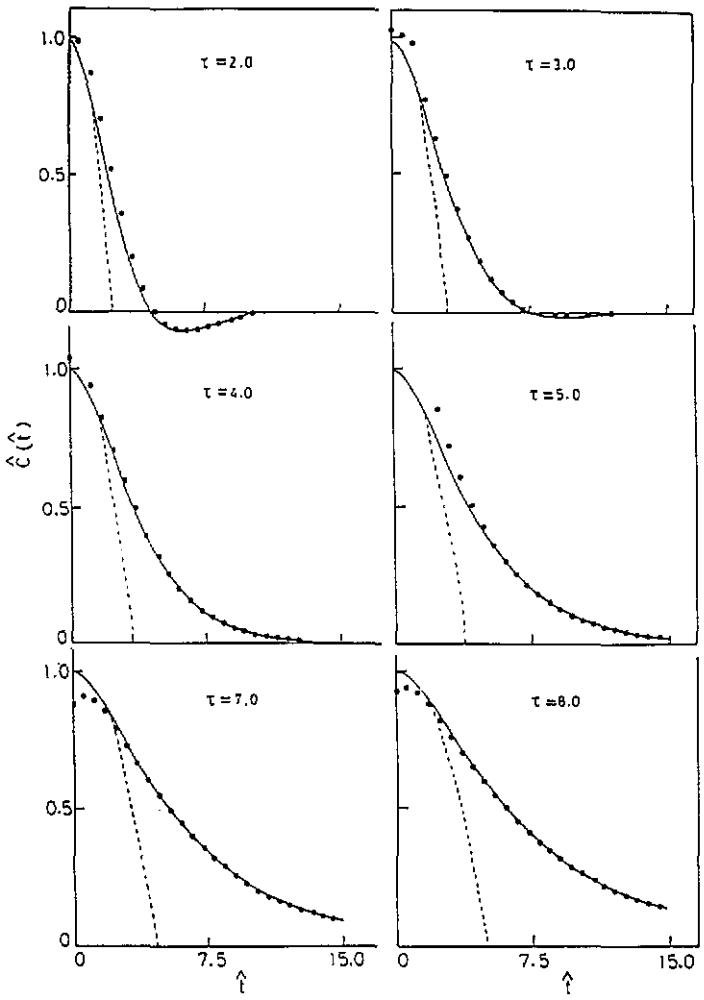

Figure 4. Numerically determined time correlation function $C(t)$ in comparison with the short-time expansion (broken curve, (21)) and the long-time expansion (solid circles, (22)) for different values of τ.

7. Comparison among sech(t), Gaussian and exponential memory functions

We compare the results for $C(t)$ obtained by using sech(t), a simple exponential and a Gaussian form of the memory function. It is found that common features of the ACF discussed by Denner and Wagner [14] for exponential and Gaussian memory are also exhibited by sech(t) memory. These features are summarized as follows. There exist two poles z_1 and z_2 that determine the long-time behaviour of the ACF. For all three memory functions, a critical value of the parameter τ_c exists which separates the regime of oscillatory behaviour from that of monotonic decay of the ACF. For $\tau \to \infty$, one of the poles tends to zero and this dominates the long-time behaviour of the ACF. However, there are differences among sech(t), exponential and Gaussian memories. These are as follows. The poles $\mathrm{Re}\, z_{1,2}$ vary with τ for $\tau < \tau_c$ for Gaussian and hyperbolic secant memories, whereas these have a fixed value of -0.5 for the exponential memory. On the other hand, for increasing

$\tau > \tau_c$ the pole $z_2(\tau)$ approaches -1 for both exponential and sech(t) memories, whereas it tends to $-\infty$ for Gaussian memory. It is also found that the poles show symmetry around $z = -0.5$ for exponential memory, whereas this kind of symmetry is totally absent in the case of Gaussian memory. On the other hand, the poles are more or less symmetric for the hyperbolic secant memory. Thus, the hyperbolic secant model memory function has some common features with the Gaussian and some with the exponential memory.

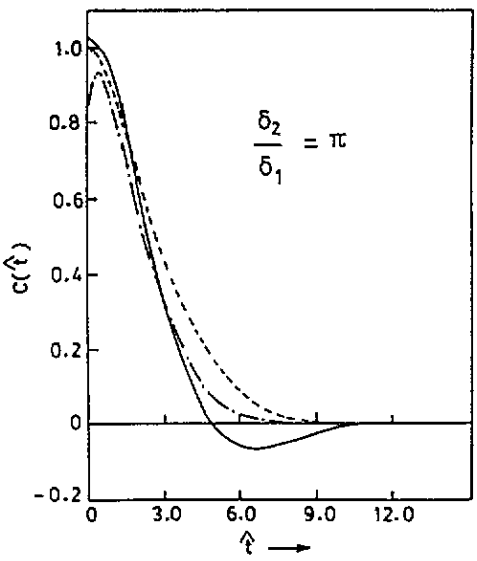

Figure 5. Comparison of time evolution of the ACF among Gaussian, hyperbolic secant and exponential memory approaches for parameter $\delta_2/\delta_1 = \pi$: solid line, sech(t) memory; dash-dot, Gaussian memory; dashed line, exponential memory.

In order to see the difference in the behaviour of the time evolution of the correlation function using different memory functions we have plotted $C(t)$ for exponential, Gaussian and sech(t) memories in figure 5 for $\delta_2/\delta_1 = \pi$. It can be seen from figure 5 that the decay of $C(\hat{t})$ with exponential and Gaussian memory is slower than that with sech(t) memory. It is also found that $C(\hat{t})$ attains a negative minimum (back scattering effect) for $\hat{t} \simeq 7.5$ for hyperbolic secant memory, whereas it remains positive for Gaussian and exponential memory functions. The above differences in these different cases can be understood by noting that $\tau = \delta_2/\delta_1$ and $\tau_c = 4$, $\tau = (2/\sqrt{\pi})\delta_2/\delta_1$ and $\tau_c = 3.811$ and $\tau = (2/\pi)\delta_2/\delta_1$ and $\tau_c = 4.4$ for exponential, Gaussian and hyperbolic secant memory, respectively. Here τ_c separates the regime of oscillatory behaviour of $C(t)$ from its monotonic decay. From this we find that $C(t)$ will show oscillatory behaviour for $\delta_2/\delta_1 < 4$, 3.37 and 6.711 for exponential, Gaussian and sech(t) memory functions, respectively. Therefore, it is seen that the back scattering effects are more pronounced for hyperbolic secant memory than for the Gaussian and exponential memories. Thus, our hyperbolic secant memory function reflects more non-linearity, which arises due to the effect of the surroundings on the atomic motion in a dense medium. Similarly, for the power spectrum $G(\omega)$ of $C(t)$, we find that a non-zero ω peak appears for sech(t) memory when $\delta_2/\delta_1 < 3.27$, whereas it appears when $\delta_2/\delta_1 < 1.887$ for the Gaussian case. The parameter τ of the sum rules up to fourth order of almost all ACFs are known [11, 16]. Therefore, our study is expected to be quite useful as one can now obtain information about the nature of decay of the ACF simply by knowing the value of the parameter and without actually solving Mori's equation numerically.

8. Conclusion

In this paper we have obtained an analytical solution of Mori's integro-differential equation for the ACF using a hyperbolic secant form of the memory function. We find that the long-time expansion (22) together with the short-time expansion (21) provides a good description of $C(t)$ for the whole time domain. We have found that the behaviour of the ACF depends on a single parameter τ, which determines whether the ACF decays in an oscillatory or non-oscillatory fashion. This parameter τ is related to the frequency sum rules of the ACF up to fourth order. Similarities as well as differences in the time evolution of $C(t)$ have been discussed for exponential, hyperbolic secant and Gaussian approaches of the memory function. It is found that back-scattering effects are more pronounced in our sech(t) memory than in Gaussian and exponential memory functions. This implies that our model reflects more non-linearity, which arises due to the effect of the motion of a molecule on its surroundings in a dense medium and its reflection on the motion of the molecule.

Acknowledgments

This work was developed at Chandigarh, India and finalized at ICTP, Trieste, Italy. One of us (KT) would like to thank Professor Abdus Salam, the International Atomic Energy Agency and UNESCO for hospitality at the International Centre for Theoretical Physics during the Condensed Matter Workshop 1993. KT also gratefully acknowledges the partial financial assistance provided by CSIR, New Delhi.

Appendix

In order to obtain the analytical expression for the poles of $\tilde{C}(z)$ for the $\tau < \tau_c$ region, we first derive a general relation between real and imaginary parts of the poles. To this end we decompose $f(z)$ into real and imaginary parts by substituting $z = x + iy$ in (23). This provides

$$x(\tau) = -(2/\pi)g_1(x, y) \tag{A1}$$

$$y(\tau) = -(2/\pi)g_2(x, y) \tag{A2}$$

where

$$g_1(x, y) = \int_0^\infty \operatorname{sech}(\hat{t}) \exp(-x\hat{t}) \cos(y\hat{t})\, d\hat{t} \tag{A3}$$

and

$$g_2(x, y) = -\int_0^\infty \operatorname{sech}(\hat{t}) \exp(-x\hat{t}) \cos(y\hat{t})\, d\hat{t}. \tag{A4}$$

(i) $\tau \leqslant \tau_c$. For $\tau \to \tau_c$ and hence for $x \to x_c$ it may be shown that the imaginary part y tends to zero. Therefore, the behaviour of the poles for $\tau \leqslant \tau_c$ can be investigated by expanding expressions (A3) and (A4) in powers of y up to terms of order y^3. Expanding (A1) we find that

$$x\tau + \frac{2}{\pi}\beta\left(\frac{x+1}{2}\right) - \frac{y^2}{4\pi}\beta''\left(\frac{x+1}{2}\right) = 0 \tag{A5}$$

and

$$y^2 = \left\{4\pi\left[x\tau + \frac{2}{\pi}\beta'\left(\frac{x+1}{2}\right)\right] \Big/ \beta''\left(\frac{x+1}{2}\right)\right\}. \tag{A6}$$

If we expand (A2) in terms of y we find that

$$y^2 = 24\pi\left[\tau + \frac{\beta'}{\pi}\left(\frac{x+1}{2}\right)\right] \Big/ \beta'''\left(\frac{x+1}{2}\right). \tag{A7}$$

Equating (A6) and (A7) in the limit $x \to x_c$ we obtain

$$x = \tau_c x_c/\tau + (\tau - \tau_c)/\tau K' \tag{A8}$$

with

$$K' = \beta'''\left(\frac{x_c+1}{2}\right) \Big/ 6\beta''\left(\frac{x_c+1}{2}\right). \tag{A9}$$

The imaginary part y, however, can be obtained directly from equation (A7) in the limit $x \to x_c$. We obtain

$$y = \left(\frac{24\pi(\tau - \tau_c)}{\beta'''[(x_c+1)/2]}\right)^{1/2}. \tag{A10}$$

(A8) and (A10) determine the real and imaginary parts of the poles for the region $\tau \leqslant \tau_c$.

(ii) $\tau \to 0$. Taking $x = 0$ in (A1) and (A2) it may be shown that for $\tau = 0$, the poles are located on the imaginary axis at $y = \pm\infty$. The behaviour of the poles in the $\tau \to 0$ limit, therefore, can be investigated from (A1) and (A2) in the limits $x \to 0$ and $y \to \pm\infty$. In the zeroth-order approximation we obtain

$$y(\tau) = -1/\tau \tag{A11}$$

and

$$x(\tau) = -(1/\tau)\ \mathrm{sech}(\pi/2\tau). \tag{A12}$$

These equations determine the poles in the $\tau \to 0$ limit.

References

[1] Heyes D M 1988 *Phys. Rev.* B **37** 5677
[2] Vogelsang R, Hoheisel C and Ciccotti G 1987 *J. Chem. Phys.* **86** 6371
[3] Heyes D M 1983 *J. Chem. Soc. Faraday Trans.* II **79** 1741; 1984 *J. Chem. Soc. Faraday Trans* II **80** 1363
[4] Levesque D and Verlet L 1987 *Mol. Phys.* **61** 143
[5] Ladd A J C, Edward Alley E and Alder B J 1987 *J. Stat. Phys.* **48** 1147
[6] Hammonds K D and Heyes D M 1988 *J. Chem. Soc. Faraday Trans.* II **84** 705
[7] Boon J P and Yip S 1980 *Molecular Hydrodynamics* (New York: McGraw-Hill)
[8] Tankeshwar K, Dubey G S and Pathak K N 1988 *J. Phys. C: Solid State Phys.* **21** L811
[9] Tankeshwar K, Pathak K N and Ranganathan S 1990 *Phys. Chem. Liq.* **22** 75
[10] Pathak K N and Tankeshwar K 1990 *Correlation in Electronic and Atomic Fluids* ed P Jena, R Kalia, P Vashishta and M P Tosi (Singapore: World Scientific)
[11] Tankeshwar K, Pathak K N and Ranganathan S 1989 *J. Phys. C: Solid State Phys.* **20** 1618; 1989 *J. Phys.: Condens. Matter* **1** 6193
[12] Heyes D M and Powles J G 1990 *Mol. Phys.* **71** 781
[13] Leegwater J A 1991 *J. Chem. Phys.* **94** 7402
[14] Denner V and Wagner M 1984 *J. Chem. Phys.* **81** 5034
[15] Grodshteyn I S and Ryzhik I M 1965 *Table of Integrals Series and Products* (New York: Academic)
[16] Bansal R and Pathak K N 1974 *Phys. Rev.* A **9** 2773; 1977 *Phys. Rev.* A **15** 2519